Quantum Membrane Accelerometer Microchip

Stefanos Andreou,[1,2] Markus Aspelmeyer,[3,4] Simon Gröblacher,[2,*] and Richard A. Norte[1,2,†]

[1] *Department of Precision and Microsystems Engineering, Delft University of Technology, Mekelweg 2, 2628CD Delft, The Netherlands*
[2] *Kavli Institute of Nanoscience, Department of Quantum Nanoscience, Delft University of Technology, Lorentzweg 1, 2628CJ Delft, The Netherlands*
[3] *Vienna Center for Quantum Science and Technology (VCQ), Faculty of Physics, University of Vienna, Boltzmanngasse 5, 1090 Vienna, Austria*
[4] *Institute for Quantum Optics and Quantum Information (IQOQI), Boltzmanngasse 3, 1090 Vienna, Austria*

(Dated: August 31, 2020)

We design an opto-mechanical accelerometer aiming to work at the precision-limits imposed by quantum mechanics. Our chip-based approach combines state-of-the-art nano-fabrication and photonics in order to pioneer new types of sensors at telecom wavelengths. In our project, we have designed a novel photonic crystal structure attached to a test mass made of silicon nitride (Si_3N_4), that allow us to confine light into small volumes and make it possible to measure movements on the femtometer scale. This proof-of-principle demonstration will allow us to realize orders-of-magnitude better acceleration sensitivities and bandwidths compared to currently available commercial sensors.

A. Introduction

To date, sensing technologies typically used in cell phones, air travel, space flight, and cars are comprised of electric, magnetic, piezo-resistive, piezo-electric and/or capacitive read-out circuits, among others [1–3]. While these read-outs allow one to reach impressive sensitivities and efficiencies, they are limited by classical and external noise, amongst other constraints. Next-generation devices will require significantly better sensitivity than is currently possible, ideally reaching the ultimate limits posed by quantum physics. In addition, several applications require sensors that are immune to electro-magnetic stray fields commonly present in the environment found within MRI scanners, electric vehicle motors, bottom-hole assemblies for drills, and any electromagnetic pulses generated by natural and industrial tools [4, 5]. In this project, we aim at developing a new on-chip accelerometer based on quantum opto-mechanical structures [6]. Opto-mechanical sensors are inherently immune to external electro-magnetic fields thus making them excellent candidates for next generation chip-based acceleration sensors. They also promise unprecedented sensitivities through quantum limited optical read-out of mechanical motion [7] which is fully integrated on a chip and readily compatible with existing semiconductor processing infrastructures.

B. Operating at Quantum Limits

The resolution of an accelerometer is fundamentally limited by its thermal noise, i.e. Brownian motion of the test-mass. This noise can be expressed as [8]

$$a_{th} = \sqrt{4\omega_m k_B T/mQ_m} \tag{1}$$

where ω_m is the resonant mechanical angular frequency of the sensor, m its mass, Q_m the mechanical quality factor, T its absolute temperature, and k_B the Boltzmann constant. Evidentially to improve the resolution of such a sensor one should strive to maximize the $m \cdot Q_m$ and minimize ω_m and T. From a commercial point of view, operating at cryogenic temperatures therefore minimizing T is not favorable while ω_m is typically tailored to the desired bandwidth of a specific application. Maximizing the product $m \cdot Q_m$ is therefore the best way forward.

During our experimental research efforts, which focus on developing opto-mechanical devices for quantum experiments at room temperature [6, 9], we have demonstrated the best on-chip force sensors currently available under these temperature conditions. The remarkably high mechanical quality factors $Q_m > 10^8$ are possible due to the devices being fabricated from stoichiometric silicon nitride with high-tensile stress of around 1 GPa. Mechanical energy loss can further be reduced by incorporating isolating phononic crystal structures [10]. Additionally this integration strategy allows for scaling the test-mass in order to reduce the thermal noise limit a_{th}. While this affects the sensor bandwidth, it has been shown that this can also be compensated by proper design [11].

Using our approach, we aim at reaching resolutions $< 1\ \mu g/Hz^{1/2}$, where g = 9.81 m/s^2 is the acceleration of gravity on earth, while maintaining a bandwidth of several tens of kHz. This is a unique combination of the specific technology as the trade-off of existing commercial accelerometers between resolution and bandwidth is very typical [12, 13] due to low Q_m, which requires large masses m necessary to achieve a certain resolution. This trade-off is further apparent by looking at the resolution/bandwidth specifications of accelerometers across different markets, from smart-phone sensors with high

* s.groeblacher@tudelft.nl
† r.a.norte@tudelft.nl

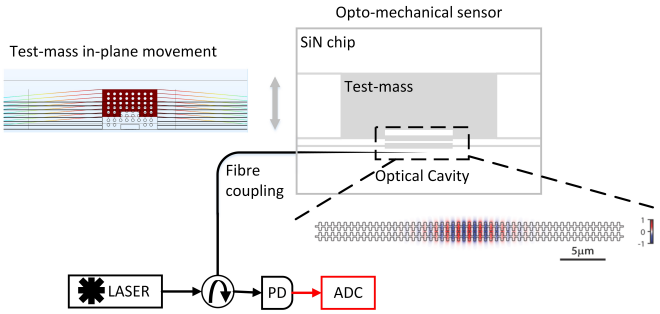

FIG. 1. Schematic illustrating the simplest form of an all-optical read-out of the opto-mechanical accelerometer. The sensor itself consists of a suspended test-mass which moves in-plane, directly changing the resonant condition of the photonic crystal cavity. The optical mode resides mostly in the gap between the two gratings and the gap is modified as the test-mass moves due to inertial forces.

bandwidth but poor resolution to defense and navigation, where orders of magnitude better resolutions are achieved at the expense of much lower bandwidths [14].

In addition to these advantages, the interrogation of our acceleration sensor is based on probing with an infrared single-mode laser. The temporal coherence of mature infrared lasers will allow us to operate at the quantum limit. This means that no classical noise but only the vacuum fluctuations of the optical field will be added to the read-out, which is the minimally achievable sensitivity in principle [15]. The processing of the optical sensor read-out is then implemented in the electrical domain using standard commercially available components such as photo-detectors and analogue-to-digital converters.

A simplified schematic of our system and its basic principles is shown in Fig. 1. The on-chip opto-mechanical structure is comprised of a fully suspended test-mass anchored to the chip via several thin tethers, with an optical cavity partly attached to the test-mass. This photonic crystal (PhC) cavity is comprised of two periodical structures in close proximity, which force the electric field to be mostly confined in the gap between them. This geometry is often called a zipper cavity [16]. The PhC, so-called fish-bones [6], confine the light also in the horizontal direction (propagation direction) by introducing a defect region. The optical resonance is designed to be in the telecom band around 1550 nm. The bottom part of the cavity experiences much smaller displacements and at much higher mechanical frequencies (MHz range). Inertial forces will cause the test-mass to move in the chip-plane, i.e. in-plane, direction therefore changing the resonant conditions. This interaction is quantified through the opto-mechanical coupling coefficient. The subsequent shift of the optical resonance can be probed by an external laser and analyzed by looking at its reflection. In-loop measurements are preferable such as balanced-detection or homodyne-detection which will be explained later. In Fig. 1 an out-of the-loop method is shown for simplicity.

C. Fabrication - High yield and scalability

Silicon nitride membranes have been fabricated and utilized in the past as force sensors [9, 11, 17], but standing problems have been their reliability, yield and long processing time mainly due to incorporated wet-etching techniques. In our approach, we only use dry etching thus minimizing the under-etching time from hours to minutes, while rendering critical point drying redundant. The latter step is essentially a hurdle to high yield as surface tensions and van der Waals forces can cause suspended structures to collapse, fracture or stick together [18, 19].

In our process, we start from 1×1 cm^2 dies of 0.5 mm silicon and an LPCVD deposited 350 μm high-stress (1.3 GPa) SiN film. We pattern the SiN using electron beam lithography and a CHF_3 plasma etch. After removing the resist and cleaning the sample with piranha solution and hydrofluoric acid, the structures are released by under-etching the silicon using SF_6 plasma etching.

A microscope image of a fabricated device is shown in Fig. 2. The test-mass has dimensions of 150×80 μm^2. The circles on the test-mass have been placed in order to assist the silicon etching below. The silicon etching, which takes about 60 s, causes some under-etching of the silicon around the structure as well. In this device there are 32 tethers on each side of the test-mass, 200 μm long, while structures with only 2 and up to 600 μm length have also been successfully fabricated (not shown). We have further scaled the tether width from between 100 nm to 1 μm, demonstrating our ability to access a large parameter space required for tailoring the accelerometer properties. The curved waveguide in the bottom facilitates efficient light coupling by using a tapered standard single-mode fiber.

D. Experimental setup

One of the critical tasks of this project has been the development of a setup to properly characterize our opto-mechanical structures and demonstrated quantum-limited acceleration detection. A schematic of the current setup is illustrated in Fig. 3.

The structure is placed on a micro-positioner in a vacuum chamber where we can reach pressures down to low 10^{-8} mbar. Light is coupled in and out using a tapered fiber as aforementioned with high efficiencies, typically larger than 60%. We use a commercial tuneable laser as a light source and couple light after a variable optical attenuator (VOA) and a circulator. The light polarization is TE as the on-chip optical cavity is designed for this polarization. The reflection is measured using a photodetector and an analogue-to-digital converter (ADC). In Fig. 3 a balance detection scheme is also shown, where the reflected light is fed to an auto-balanced detector along with an attenuated version of the laser output. This will allow us to perform measurements in which the relative intensity noise of the laser is greatly suppressed while ensuring

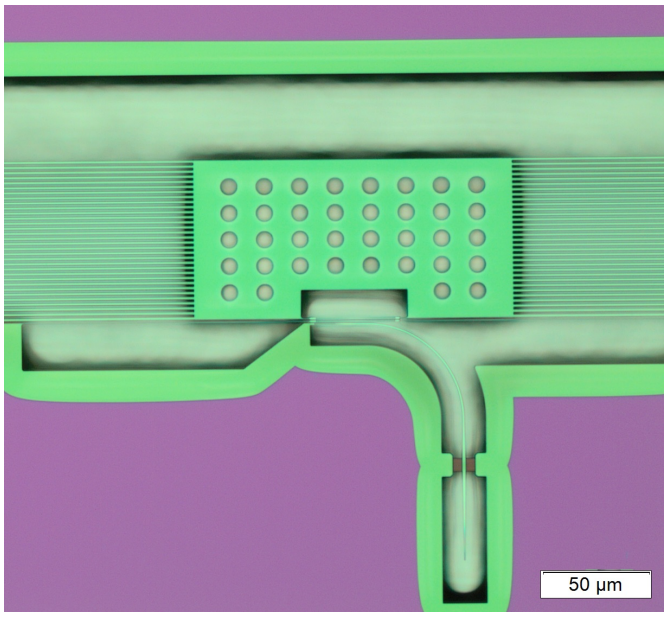

FIG. 2. Microscope image of a fabricated accelerometer. The test-mass, zipper cavity and optical waveguides are fully suspended. In this particular device, the test-mass is tethered to the chip via 32 tethers on each side. The waveguide on the bottom of the figure uses inverse tapering for efficiently coupling light to the optical cavity through a tapered fiber.

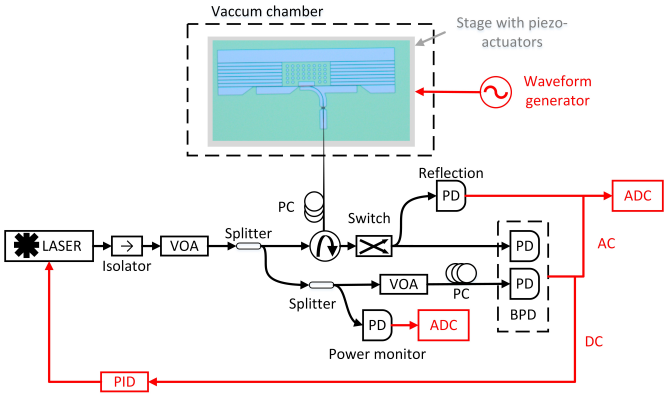

FIG. 3. Experimental setup.

good long-term stability through a simple locking of the laser onto the optical resonance slope. Additional, further improvements to reach quantum limited read-out can be implemented through a homodyne-detection scheme.

Furthermore, piezo-actuators have been installed in order to excite the opto-mechanical accelerometer in different axes. Commercial accelerometers are also being deployed in order to calibrate the acceleration sensitivity, which remains on-going work.

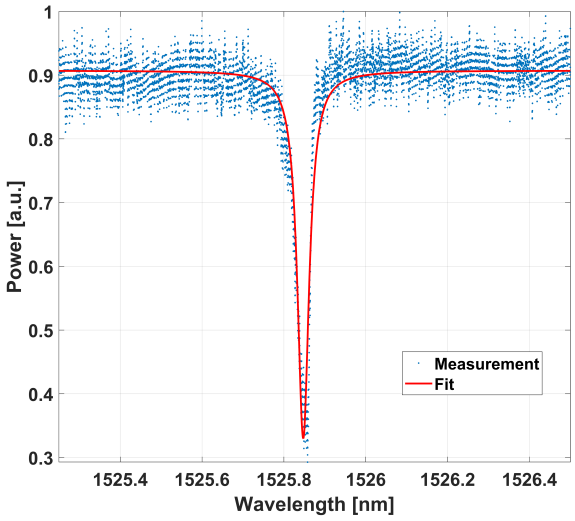

FIG. 4. Measured reflection (blue) and fitted spectrum (red) of the photonic crystal cavity in the telecom band. The FWHM of the cavity is 4.3 GHz corresponding to $Q_{opt} = 4.5 \times 10^4$.

E. Results

A typical reflection spectrum of a PhC cavity is shown in Fig. 4. The $\kappa/2\pi$ is 4.3 GHz, corresponding to an optical quality factor Q_{opt} of about 4.5×10^4. The optical cavity is designed to be over-coupled therefore we estimate intrinsic κ_{in} and extrinsic κ_{ex} linewidths of 0.9 GHz and 3.4 GHz, respectively.

The mechanical properties of one of the fabricated devices are initially retrieved by the Brownian motion of the test-mass and by aligning the laser onto the blue-detuned side of the resonance. An example of the mechanics recorded with an electrical spectrum analyzer is shown in Fig. 5. The device has four tethers on each side of the test-mass, 600 μm long and 0.75 μm wide. The test-mass has a mass of about 10^{-12} kg. The two subplots show the power spectral densities of the reflected signal for an input power of about 10 μW. In Fig. 5(a) modes are only present above 80 kHz. A closer look in Fig. 5(b) reveals three modes. Based on our simulations we conclude that the three modes at 78.5 kHz, 80.5 kHz and 97.8 kHz correspond to the out-of-plane, in-plane and torsional modes of the test-mass, respectively. This is supported by measurements taken using a vibrometer as well. We would like to mention that the mechanical frequencies are slightly lower than expected, which is attributed to the underetching of the silicon around the structures visible in Fig. 2.

The widths of the peaks in Fig. 5 are resolution limited (<1 Hz), indicating that the mechanical quality factors are larger than 10^5. Proper measurements of Q_m are to be performed soon, with preliminary measurements confirming a Q_m on the order of 10^6. Conservative calculations with such quality factors for the opto-mechanical accelerometer indicates a thermal noise < 30 μg with sub-

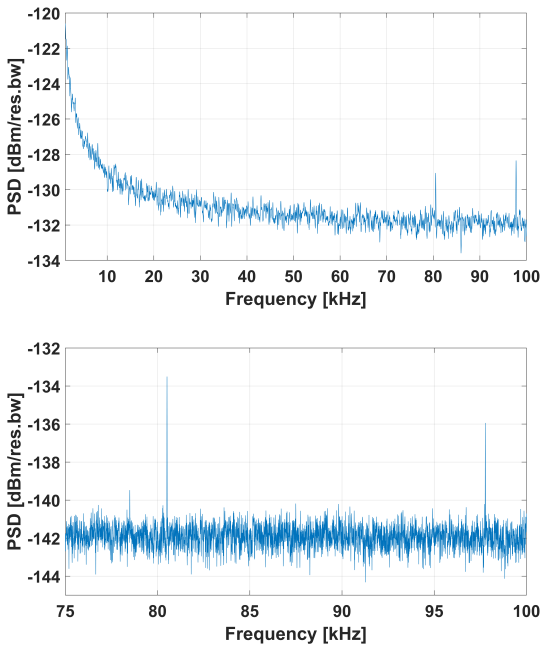

FIG. 5. Power spectral density of the reflected signal for (a) a wide scanning range with 100 Hz resolution bandwidth and (b) narrow scanning range with 10 Hz resolution bandwidth. The modes at 78.5 kHz, 80.5 kHz and 97.8 kHz correspond to the out-of-plane, in-plane and torsional modes of the test-mass, respectively, in good agreement with our simulations.

μg resolutions being within reach.

F. Conclusions and outlook

We have demonstrated the reliable fabrication of opto-mechanical chip-based accelerometers with a simple fabrication process and access to a large design parameter space, while our characterization setup and demonstrator are being finalized. We demonstrate high optical quality factors on the order of several times 10^4 and the first measurements indicate mechanical quality factors in excess of 10^6, which leads to very promising estimates for a sub-μg thermal noise-floor and the envisioned resolutions being within reach for bandwidths of tens of kHz. Full characterization of the quantities of interest, e.g. accurate mechanical quality factors and opto-mechanical coupling, are currently being performed. With these we will be able to quantify the resolution of our system and further optimize our system through appropriate design choices.

Acknowledgements

We would like to thank Gary Steele and Peter Steeneken for early support of the project. This work is part of ATTRACT that has received funding from the European Union's Horizon 2020 Research and Innovation Programme. We further acknowledge support from an NWA Startimpuls grant on "Inertial Quantum Navigation".

[1] N. Barbour and G. Schmidt, IEEE Sensors Journal **1**, 332 (2001).
[2] N. Yazdi, F. Ayazi, and K. Najafi, Proceedings of the IEEE **86**, 1640 (1998).
[3] S. Tadigadapa and K. Mateti, Measurement Science and Technology **20**, 092001 (2009).
[4] H. Nakstad and J. T. Kringlebotn, Nature Photonics **2**, 147 (2008).
[5] G. K. A. G. Krishnan C. U. Kshirasgar and N. Bhat, J. Indian Inst. Sci. **87**, 333 (2007).
[6] J. Guo, R. Norte, and S. Gröblacher, Phys. Rev. Lett. **123**, 223602 (2019).
[7] G. Anetsberger, E. Gavartin, O. Arcizet, Q. P. Unterreithmeier, E. M. Weig, M. L. Gorodetsky, J. P. Kotthaus, and T. J. Kippenberg, Phys. Rev. A **82**, 061804 (2010).
[8] K. Y. Yasumura, T. D. Stowe, E. M. Chow, T. Pfafman, T. W. Kenny, B. C. Stipe, and D. Rugar, Journal of Microelectromechanical Systems **9**, 117 (2000).
[9] R. A. Norte, J. P. Moura, and S. Gröblacher, Phys. Rev. Lett. **116**, 147202 (2016).
[10] A. H. Safavi-Naeini and O. Painter, Opt. Express **18**, 14926 (2010).
[11] A. G. Krause, M. Winger, T. D. Blasius, Q. Lin, and O. Painter, Nature Photon. **6**, 768 (2012).
[12] F. Guzmán Cervantes, L. Kumanchik, J. Pratt, and J. M. Taylor, Applied Physics Letters **104**, 221111 (2014), https://doi.org/10.1063/1.4881936.
[13] K. McConnell and P. Varoto, *Vibration Testing: Theory and Practice* (Wiley-Interscience, 2008).
[14] "Choosing the most suitable mems accelerometer for your application," https://www.analog.com/media/en/analog-dialogue/volume-51/number-4/articles/choosing-the-most-suitable-mems-accelerometer-for-your-application-part-1.pdf (2017).
[15] O. Gerberding, F. G. Cervantes, J. Melcher, J. R. Pratt, and J. M. Taylor, Metrologia **52**, 654 (2015).
[16] M. Eichenfield, R. Camacho, J. Chan, K. J. Vahala, and O. Painter, Nature **459**, 550 (2009).
[17] C. Reinhardt, T. Müller, A. Bourassa, and J. C. Sankey, Phys. Rev. X **6**, 021001 (2016).
[18] A. G. Krause, *Acceleration Sensing, Feedback Cooling, and Nonlinear Dynamics with Nanoscale Cavity-Optomechanical Devices* (California Institute of Technology, 2015).
[19] R. A. Norte, *Nanofabrication for On-Chip Optical Levitation, Atom-Trapping, and Superconducting Quantum Circuits* (California Institute of Technology, 2015).